JOTCS A
Journal of the Turkish Chemical Society
Section: A
Chemistry
TURKISH CHEMICAL SOCIETY

Heteroleptic Transition Metal Complexes of Eflornithine Hydrochloride Monohydrate: Synthesis, Characterization, *in silico* and *in vitro* Biological Studies

Wahab A. Osunniran[1]* , Yusuf O. Ayipo[1,3], Abdullahi O. Rajee[2], Adebayo T. Bale[1], Mercy O. Bamigboye[4], and Joshua A. Obaleye[2]

[1]Mus Alparslan University, Department of Math, Mus, Turkey
[1]Kwara State University, Department of Chemistry and Industrial Chemistry, Malete, P.M.B 1530, Ilorin, Nigeria.
[2]University of Ilorin, Department of Chemistry, P.M.B 1515, Ilorin, Kwara State, Nigeria
[3]Universiti Sains Malaysia, Centre for Drug Research, Pulau, 11800 USM, Pinang, Malaysia.
[4]University of Ilorin, Department of Industrial Chemistry, Ilorin, Kwara State, P.M.B 1515, Nigeria

Abstract: Incessant development of resistance to drugs by microorganisms remains a major setback associated with the currently available antibiotics, thereby making imperative a continuous search for alternative candidates with improved efficacy. Previous studies have shown enhanced antimicrobial activity of some bioactive molecules upon coordination with metal ions. Thus, in this study, Cu(II), Co(II), and Ni(II) complexes of eflornithine hydrochloride monohydrate (EHM) were synthesized and probed for bactericidal activity via *in vitro* and *in silico*. The characterization results such as CHN analysis, FTIR, UV-visible magnetic susceptibility and Electrospray Ionization Mass Spectrometry (ESI-MS) reveal that EHM coordinates as a bidentate ligand to each central metal ion in the molar ratio 1:2 through O and N in the COO^- and NH_2 group respectively, and also suggest octahedral geometry in each complex. The physicochemical and pharmacokinetics parameters predicted *in silico* support the bio-applicability and safety of the complexes. From the *in vitro* antibacterial study, the complexes demonstrate improved activity against *Staphylococcus aureus*, *Escherichia coli,* and *Pseudomonas aeruginosa* with an average minimum inhibitory concentration (MIC) of 0.01 mg/L similar to ciprofloxacin, compared to EHM whose MIC >1.00 mg/L. Although, not all the complexes satisfy Lipinski's drugability rule of 5 due to their molecular weight, however, coordination with metal ions improves the biological activities of EHM and the complexes demonstrate potential for further transformation into antibiotic therapeutics.

Keywords: Bioinorganic coordination chemistry, antibiotics, gram positive and negative bacteria, eflornithine, drug resistance.

Submitted: July 08, 2022. **Accepted:** September 20, 2022.

Cite this: Osunniran WA, Ayipo YO, Rajee AO, Balee AT, Bamigboye MO, Obaleye JA. Heteroleptic Transition Metal Complexes of Eflornithine Hydrochloride Monohydrate: Synthesis, Characterization, in silico and in vitro Biological Studies. JOTCSA. 2022;9(4):1309–22.

DOI: https://doi.org/10.18596/jotcsa.1142442.

***Corresponding author. E-mail:** wahab.osunniran@kwasu.edu.ng.

INTRODUCTION

The significance of metal ions or metal ion binding components into biological systems for diagnosis and treatment of diseases is one of the focal segments in the field of bioinorganic chemistry (1). A characteristic feature of metals is that they form positively charged ions by losing electrons to become soluble in biological fluids. In this cationic forms, metals play their important roles in biological functions. Metal ions are electron deficient and a good number of biological molecules such as

proteins and DNA are electron rich. Thus, the interaction of these opposing charges leads to strong affinity between metalloproteinase-inclined metal ions and the corresponding biological targets (2). Some important biological functions are strongly dependent on the coordinated metal ion within the structures of the relevant enzymes and cofactors. Examples of such metal-organic framework for biological processes include the hemoglobin in red blood cells which contains an iron porphyrin complex for oxygen transport and storage, the chlorophyll in green plants for photosynthetic process which contains magnesium porphyrin complex, cobalt complex in the coenzyme B_{12} is essential for the transfer of alkyl groups and Vitamin B_{12} (cobaloxime), a cobalt complex containing a glyoxime ligand, and is one of the examples of a naturally occurring organometallic complex (3).

The rapid occurrence of antibiotic resistance (AR) has become a global threat which oftentimes endanger the efficacy of the available therapeutics against emerging pathogenic diseases. In addition to the resistance features constantly developed by the microbes after a prolong treatment, AR is also attributed to the abuse or misuse of the antibiotic medications as well as inadequate pharmaceutical innovations to match the meteoric transmutations and translations of the microorganism genomes (4). Thus, a coordinated research development is continuously required to manage the crisis. Inorganic compounds especially metal complexes have performed an essential role in the advancement of new metal based drugs which were found not only to have good spectrum of activity, but having novel mechanistic potentials which are amenable for overcoming AR (5). Metals not only offer templates for synthesis, but they also introduce functionalities that improve drug delivery vectors and interact favorably with metalloproteinases to accomplish biological purposes. The pharmacological activity of metal complexes is greatly dependent on the type of the metal ions and the donor sequence of the ligands since separate ligands exhibit different biological properties (5,6). Moreso, the efficacy of various organic molecules with therapeutic potentials can be enhanced upon coordination to appropriate metal ions to form complexes (7,8). The pharmacodynamics and pharmacokinetics of these complexes usually increase, with the resultant tendency to penetrate the cell membrane of the microbes. Again, the decrease in the polarity of the metal ions by partial sharing of its positive charges with the donor group of ligands have been proposed as reasons for their better efficacy over their parent compound ligands while the structural modifications favor multitarget pharmacological mechanisms to overcome AR (5).

Eflornithine hydrochloride monohydrate with molecular formula of $C_6H_{12}F_2N_2O_2.HCl.H_2O.$, an antiprotozoal agent, is a specific, irreversible inhibitor of the enzyme ornithine decarboxylase.The drug was initially formulated for use in cancer and is in phase III clinical trials for its use in preventing recurrence of superficial bladder cancer. It has been used as antiprotozoal agent in the treatment of meningoencephalic stage of trypanosomiasis caused by(African trypanosomiasis). Eflornithine has been tested for its anti inflammatory activity. Eflornithine 13.9% cream is used to inhibit growth and reduce the amount of facial hair in women. (9,10,11). This article however focuses on the potential of eflornithine hydrochloride monohydrate as antibiotic agent.

Therefore, in continuation of our studies on coordination of metal with biologically important ligands (12-14), we aim to synthesize and characterize new set of transition divalent metals (Cu(II), Co(II) and Ni(II)) complexes containing Eflornithine hydrochloride monohydrate (EHM) (Fig. 1) as ligand with different donor atoms and probe their multi-mechanistic pharmacological potentials against some drug-resistant bacterial strains.

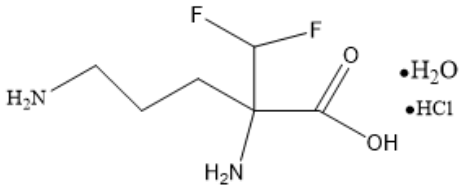


Figure 1: Molecular structure of eflornithine hydrochloride monohydrate. (11,15)

EXPERIMENTAL

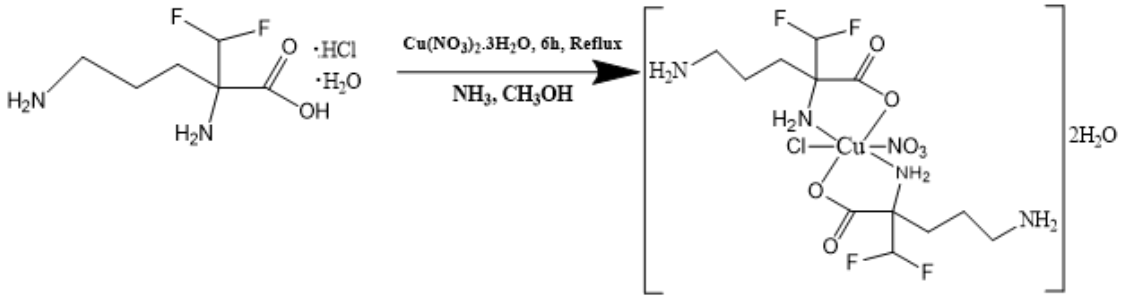
Materials

The EHM, copper(II) nitrate trihydrate, nickel(II) acetate tetrahydrate and cobalt(II) acetate tetrahydrate, silver nitrate, ammonia, methanol, and acetone were commercially obtained from British Drug House Chemical Limited Co. Poole England. Isolates of S*taphylococcus aureus*, *Escherichia coli* and *Pseudomonas aeruginosa* were cultured and obtained from the University of Ilorin Teaching Hospital through Microbiology Department, University of Ilorin, Nigeria.

Synthesis of $[Cu(EHM)_2(NO_3)(Cl)].2H_2O$ (Complex 1)

A 0.2416 g (1 mmol) of copper(II) nitrate trihydrate dissolved in 20 mL methanol with slow addition of 0.4734 g (2 mmol) of EHM in 10 mL concentrated ammonia while stirring resulted in blue colored solution. The solution was refluxed for 6 hours and left at room temperature for 8 hours after which blue precipitates were formed (Scheme 1). The progress of the reaction was monitored using TLC and melting point determination. The precipitates

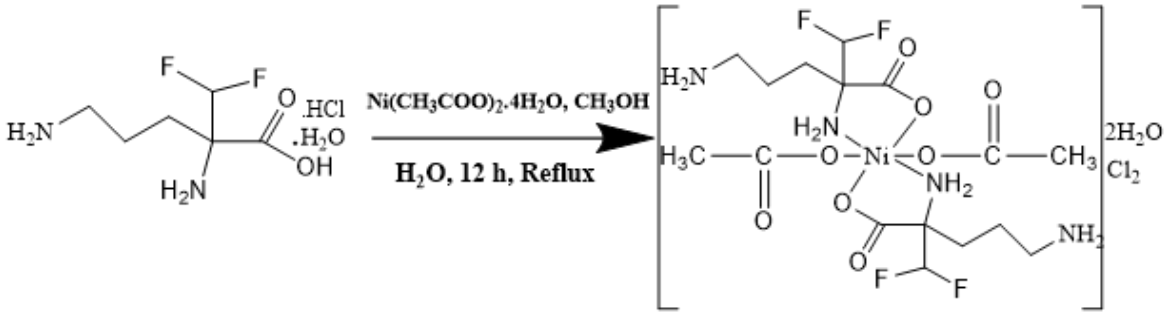
(complex) formed were separated out by filtration, washed with cold methanol and dried over silica gel in a desiccator.



Scheme 1: Synthesis of complex 1.

Synthesis of $[Ni(EHM)_2(CH_3COO)_2]Cl_2.2H_2O$ (Complex 2)

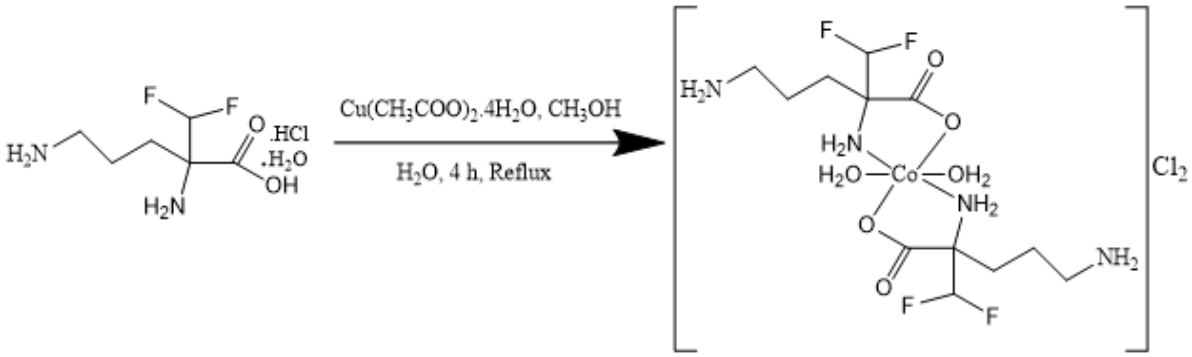
To the 10 mL aqueous solution containing 0.4734 g (2 mmol) EHM, 20 mL of methanolic solution containing 0.2489 g (1 mmol) nickel(II) acetate tetrahydrate was added under constant stirring. The resulting mixture was refluxed for 12 hours until stable green precipitates appeared (scheme 2). The progress of the reaction was monitored using TLC and melting point determination. The precipitate formed were separated out by filtration, washed thrice with cold acetone, recrystallized in water/acetone (3:1) solution and dried over silica gel in a desiccator.



Scheme 2: Synthesis of complex 2.

Synthesis of $[Co(EHM)_2(H_2O)_2]Cl_2$ (Complex 3)

A 0.4734 g (2 mmol) of EHM was dissolved in 15 mL of distilled water followed by a slow addition of 0.2491 g (1 mmol) of cobalt(II) acetate tetrahydrate previously dissolved in 10 mL of methanol. The resulting pinkish solution was then refluxed for 4 h until precipitates were formed (Scheme 3). After cooling, the product was filtered, dried and redissolved in methanol for recrystallization. The progress of the reaction was monitored using TLC and melting point determination. The recovered solution was allowed to evaporate slowly at room temperature. The purple precipitate obtained was then dried over silica gel.



Scheme 3: Synthesis of complex 3.

Preliminary test for water molecule, chloride and nitrate ions

The presence of water of crystallization within or outside the coordination sphere of each complex was assessed using cobalt chloride paper. The color change of the paper from blue to pink indicates positive. For the chloride ion outside the coordination sphere, aqueous $AgNO_3$ and NH_4OH were used for confirmation on the solution of each complex. A white precipitate soluble in excess NH_4OH indicate the presence of uncoordinated Cl^- ion. The complexes were strongly heated to qualitatively observe the fumes produced due to the presence of suspected nitrate ion from the salts.

Instrumental analyses for characterization

The elemental (CHN) analyses were carried out using micro-analytical laboratory of Medac Limited United Kingdom on Thermo Flask 112 CHNSO while FTIR spectra were measured on FTIR -8501 Shimadzu spectrophotometer over 4000-400 cm^{-1} using KBR pellets. Melting points were determined on MPA100 OptiMelt Automated Melting Point system. Solution electronic absorption spectra of the ligand as well as complexes were run in the range of 180-400 nm and 180-1100 nm respectively on Jenway 6405uv/vis. The electrospray ionization mass spectra were recorded using Micromass Autoseptic Premier/Agilent HP6890GC at Medac Limited, UK. Magnetic susceptibility measurement of the chelates of metals were determined on a Gouy balance at room temperature using $Hg[Co(SCN)_4]$ with the corrections of diamagnetic on Pascal's constants.

In silico predictions of biological activity and ADMET properties

The broad spectrum of biological activities of the synthesized complexes were predicted using the cheminformatics and bioinformatics interface of Molinspiration server (https://molinspiration.com/cgi-bin/properties) by input of SMILES file in each case. The Java tools incorporated within the server supports computational analysis through the algorithm of active training sets generation from which the cumulative bioactivity of the target molecules are predicted through their probable fragments. Each complex molecule was scored for likeliness in activity through various inhibition mechanisms on G protein-coupled receptor (GPCR), kinase, nuclear receptor and enzyme as well as ability to modulate ion channel.

The physicochemical and pharmacokinetics profiles of the complexes were predicted in terms of adsorption, distribution, metabolism, excretion and toxicity (ADMET) using the web-based Swiss ADME computational tools by inputting the SMILE file of each complex (16,17). The properties further reveal the drug-likeness of the molecules under study.

Antimicrobial screening

The in vitro antibacterial activity of the Eflornithine hydrochloride monohydrate and its metal complexes was evaluated using agar diffusion technique (18). Three clinical gram negative and gram positive bacteria, *Escherichia coli* (*E. coli*), *Staphylococcus aureus* (*S. aureus*) and *Pseudomonas aeruginosa* (*P. aeruginosa*) isolates were challenged with varying degree metal complexes and ligand concentrations. Zones of inhibition were explained using standard recommendation of Clinical and Laboratory Standards Institute, 29th Edition (19).

RESULTS AND DISCUSSION

Complex 1: M.wt: 559.36 $gmol^{-1}$; Yield: 63.2%; Elemental analysis for $Cu(EHM)_2(NO_3)(Cl)].2H_2O$ ($C_{12}H_{26}F_4N_4O_5ClCu$) calculated (found)%: C 25.77 (26.11), H 4.69 (4.70), N 12.52 (12.56); IR data (KBr, cm^{-1}): 3311, 3214, 3104, 3018, 1671, 1452, 1278, 1185, 1156, 1069, 1020, 798, 556, 530, 425. UV−vis spectrum in water (λ_{max} nm (cm^{-1})): 256 (39,063), 650(15,384). Molar Conductivity (Λ, Scm^2 mol^{-1}): 155, Magnetic susceptibitity (μ_{eff}(B.M)): 2.0

Complex 2: M.wt: 646.04 $gmol^{-1}$; Yield: 99.4%; Elemental analysis for $[Ni(EHM)_2(CH_3COO)_2]Cl_2.2H_2O$ ($C_{16}H_{32}F_4N_4O_{10}Cl_2Ni$) calculated (found)%: C 29.75 (29.99), H 4.99 (5.05), N 8.67 (8.46); IR data (KBr cm^{-1}): 3441, 3235, 3161, 1600, 1371, 1198, 1112, 1031, 771, 553, 435. UV−vis spectrum in water (λ_{max} nm (cm^{-1})): 278(35,971), 373 (26,810), 651(15,361), 991(10,091). Molar Conductivity (Λ, Scm^2 mol^{-1}): 387, Magnetic susceptibitity (μ_{eff}(B.M)): 3.29

Complex 3: M.wt: 528.19 $gmol^{-1}$; Yield 83.26%; Elemental analysis for $[Co(EHM)_2(H_2O)_2]Cl_2$ ($C_{12}H_{26}F_4N_4O_6Cl_2Co$) calculated (found) (%) : C, 27.29 (27.21); H, 4.96 (4.78); N, 10.61 (10.04). IR data (KBr, cm^{-1}): 3404, 3269, 3165, 3073, 1601, 1398, 1198, 1172, 1030, 841, 793, 565, 549, 444. UV−vis spectrum in water (λ_{max} nm (cm^{-1})): 295 (33,898), 485 (20,619), 550 (18,182), 680 (14,706). Mass Spectrum [ESI]: $[M + H + Li]^+$ m/z 537.09 (calculated), 537.10 (found) ; $[2EHM + 2H]^{2+}$ 183.09 (calculated.), 183.10 (found). Molar Conductivity (Λ, Scm^2 mol^{-1}): 362, Magnetic susceptibitity (μ_{eff}(B.M)): 4.07

From the result Table 1, the purity of the synthesized metal complexes is supported by sharp melting point ranges while the variations in comparison with the starting material (EHM) indicate changes in chemical characteristics possibly due to progress in the reaction which was confirmed using TLC. Color difference is also a contributing factor for the formation of new compounds. All the synthesized metal complexes are soluble in DMSO and water to form electrolytes but insoluble in usual organic solvents. The presence of water of crystallization outside the coordination sphere in

complexes 1 and 2 is indicated by the cobalt chloride paper. The droplets of colorless liquid stemmed out from gently heating of metal complexes (1 and 2) turned blue cobalt chloride paper pink, thus confirming the occurrence of water molecules outside the coordination sphere. The water molecules in complex 3 is complexed hence gave negative result with cobalt chloride paper. Similarly, when some drops of 0.1 M $AgNO_3$ was added to each of the metal complexes in test tube, complexes 2 and 3 gave white precipitate of AgCl soluble in excess NH_4OH confirming the presence of chloride anions outside the coordination sphere (Schemes 1 and 2), however, no precipitate was noticed in complex 1, indicating the possibility of its chloride ion in coordination to the metal ion (scheme 1). Upon strong heating, only complex 1 produced a dense reddish-brown fumes of NO_2, indicating the presence of nitrate ion in the complex (Scheme 1) while others test negative. These are supporting indications for the formation of new compounds.

Table 1: Analytical data of ligand and metal complexes.

	mp (°C)	Yield (%)	(Found) Calculated %			Color
			C	H	N	
EHM	236 – 237	--	(30.06) 30.45	(6.52) 6.39	(11.70) 11.84	White
Complex 1	202 – 204	63.2	(26.11) 25.77	(4.70) 4.69	(12.56) 12.52	Blue
Complex 2					(8.46)	
	211 – 213	99.4	(29.99) 29.75	(5.05) 4.99	8.67	Light green
Complex 3	138 – 140	83.3	(27.21) 27.29	(4.78) 4.96	(10.04) 10.61	Purple

Fourier Transform Infra-Red spectra

The characteristic FTIR bands of the metal complexes differed from the free ligand (EHM) and supplied important signals regarding the complexation and bonding sites of the ligand. Pertinent characteristic bands of the metal complexes are listed in Table 2. The principal bands attributed to asymmetric (υ_{as}) and symmetric (υ_s) stretching frequencies of OCO groups are reported in Table 3. The infrared spectrum of the ligand shows a medium intensity band at 3048 cm^{-1} assigned to υ(OH) of carboxylic acid group. On complexation with transition metal ions, this band shifted significantly, indicating possible coordination through the carboxylate oxygen atoms through deprotonation. The disappearance of this band in the spectrum of complex 2 is another proof of coordination through the site (12,14,20). This is further supported by the shifts in υ_{asy}(OCO) and υ_{sym}(OCO) as contained in Table 3. Thus, the data in Table 3 can be explored to deduce that the carboxylate groups take part in coordination to metal atom because the observable difference, $\Delta\upsilon = \upsilon_{asy}(OCO) - \upsilon_{sym}(OCO)$ in the range 148-229 characterizes the metal-carboxylate bond type. The differences between υ_{asy}(OCO) and υ_{sym}(OCO) stretching frequencies of all the metal complexes were found to be greater than that of the ligand and also greater than 200 cm^{-1} as reported in Table 3. This confirms the monodentate coordination of the carboxylate group to the central metal ion (13,21,22), in good conformity with earlier study on the same ligand where X-ray single crystal was obtained (13). The bands in the region 3254 and 3173 cm^{-1} attributable to the asymmetric and symmetric stretching frequencies of primary amine (NH_2) in the spectrum of the ligand undergo a red shift in the spectra of the complexes, indicating the involvement of NH_2 in the chelation (22,23). The observation was further strengthened by the sharp absorption band at 754 cm^{-1} in the spectrum of the ligand, due to NH_2 deformation (out-of-plane band) which moved to higher frequencies after coordination to metal ions through amino nitrogen atom. A strong band observed at 3393 cm^{-1} is assignable to stretching frequency of lattice water molecules (24–26) which shifts to higher wavenumber (3404–3441 cm^{-1}) on complexation. In the lower frequency region, new bands (non-ligand bands) with medium to weak intensities which provide direct evidence for the complexation (Metal – Ligand bond) were spotted in the spectra of the complexes in the range of 444 and 553 cm^{-1} assigned to υ(M-O)/(M-N)/(M-Cl) stretching frequencies (25, 27), while the coordination of water molecule to the metal ion in complex 3 is indicated by the $\delta(H_2O)$ at 841 cm^{-1} while similar bands in others are attributable to the $\delta(NH_2)$ (28). The shifting, disappearance or appearance of bands from the spectra of EHM to those of the complexes (Fig. 2-5) further support the argument for the formation of new compounds.

Table 2: Characteristic FTIR absorption band (cm^{-1}) of ligand and its metal complexes.

Compound	υ(OH) carboxylic	υ(NH_2) asy/sym	υ(OCO) asy/sym	υ(C-N)	υ(H_2O)	υ(M-N)/ υ(M-O)/ υ(M-Cl)	δ(NH_2)/ δ(H_2O)	υ(NO_3)
EHM	3048	3254/3173	1647/ 1499	1138	3393	-	754	-
Complex 1	3018	3214/3104	1671/ 1452	1185	3311	530,425	798	1069, 899
Complex 2	-	3235/3161	1600/ 1371	1198	3441	553,435	771	-
Complex 3	3073	3269/3165	1601/ 1398	1198	3404	549,444	841	-

Table 3: Principal IR bands (cm^{-1}) for OCO groups in ligand and metal complexes[1].

Compound	Y_{asy} (OCO)	Y_{sym} (OCO)	$\Delta\upsilon = \upsilon_{asy} - \upsilon_{sym}$
EHM	1647	1499	148
Complex 1	1671	1452	219
Complex 2	1600	1371	229
Complex 3	1601	1398	203

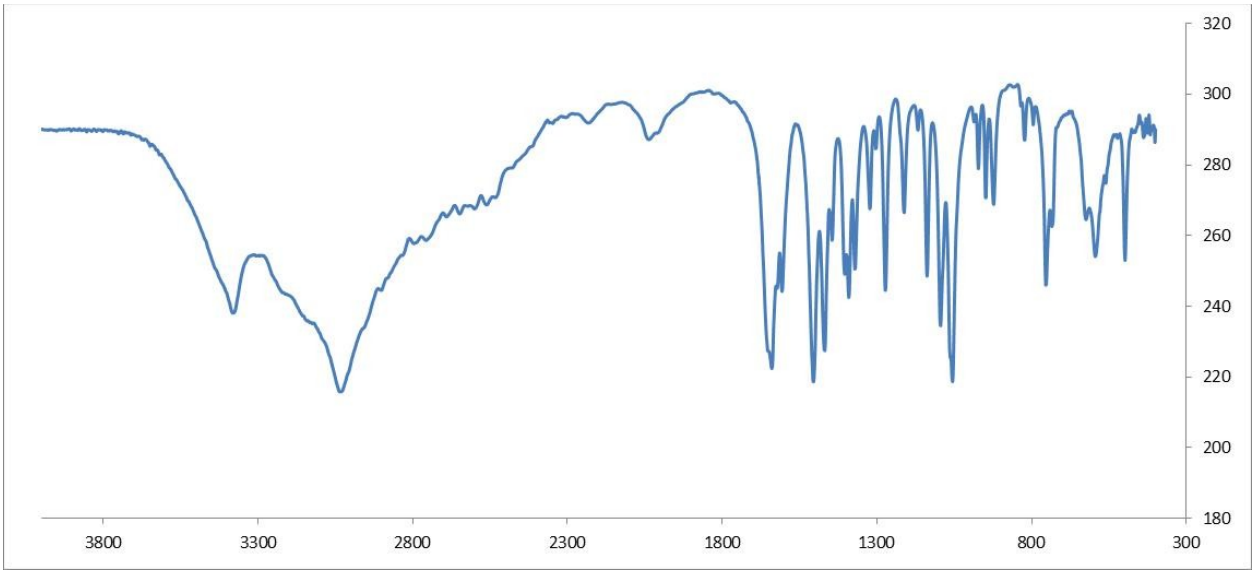


Figure 2: FTIR spectrum of the EHM (eflornithine ligand).

1 The coordination is monodentate.

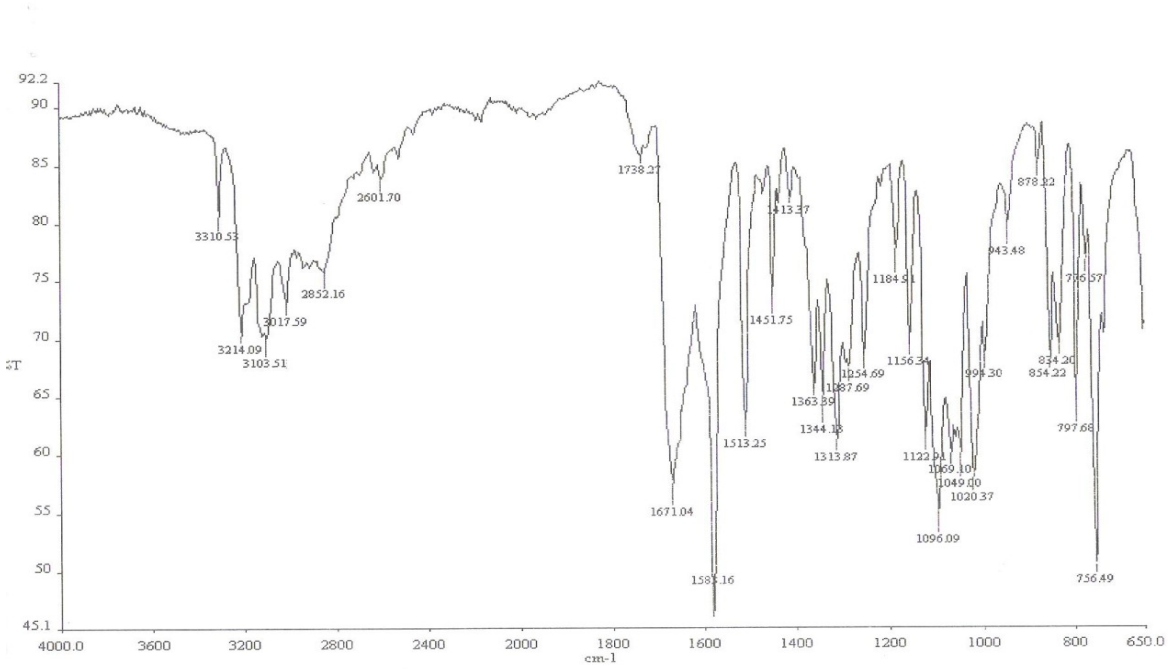


Figure 3: FTIR spectrum of the copper complex of EHM (eflornithine ligand).

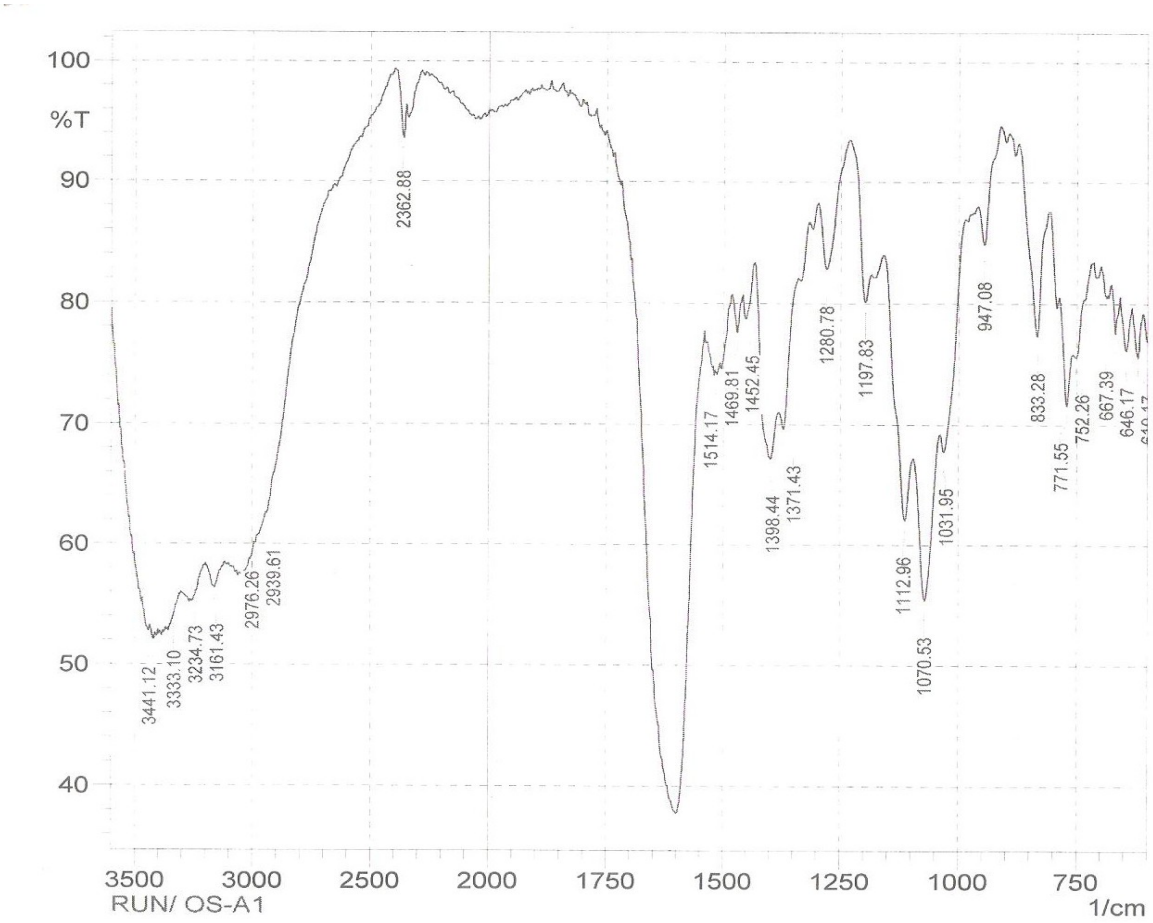


Figure 4: FTIR spectrum of the nickel complex of EHM (eflornithine ligand).

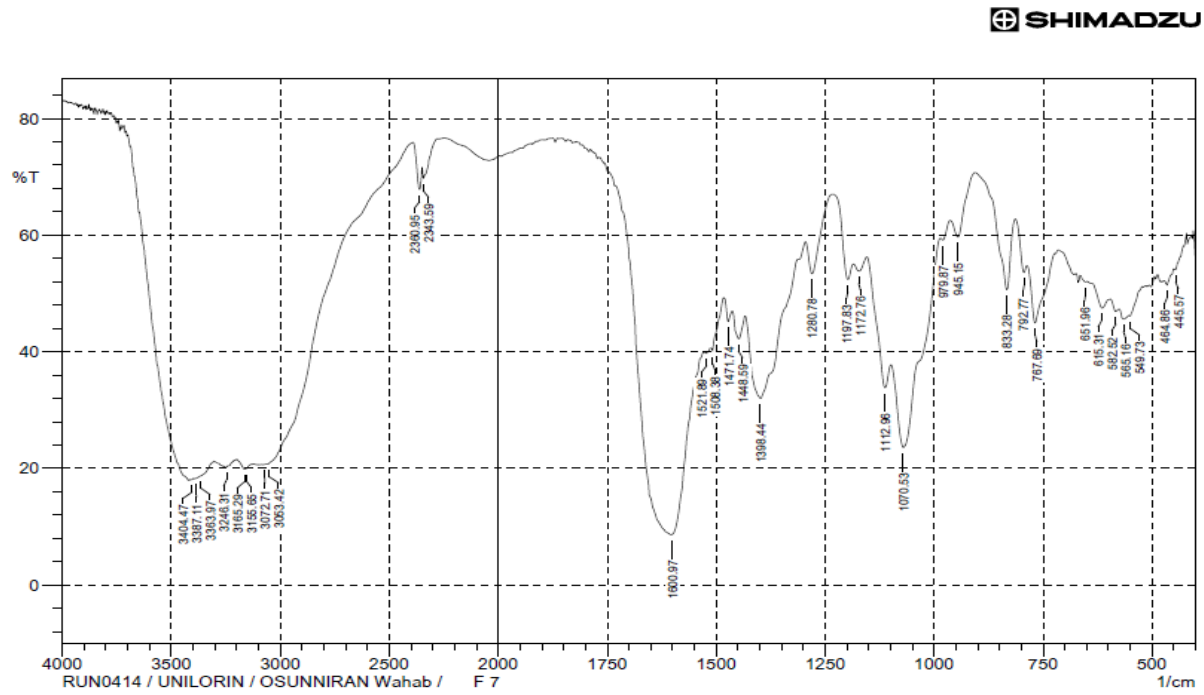


Figure 5: FTIR spectrum of the cobalt complex of EHM (Eflornithine ligand).

Electronic spectra and magnetic susceptibility

The electronic spectra data, their respective assignments/transitions and magnetic susceptibility of metal complexes were presented in Table 4. The electronic spectra of the complexes with EHM show bands in the region 256-299 nm which were assigned to n → π∗ transition due to non-bonding electrons present on the oxygen of (C=O) and nitrogen of amine group. The absorption spectra of Cu (ll) complex of EHM showed a single broad band in the visible region at 650 nm conforming to $^2E_g \rightarrow {}^2T_{2g}$ transition with an expected splitting due to the tetragonal distortion of the octahedral d^9 Cu(II) ion. For the Ni(II) complex, the absorption bands within the visible region of 651 and 991 nm corresponding to $^3A_2g \rightarrow {}^3T_1g(F)$ transition respectively. Similar absorption occurs at visible regions of 485 and 680 nm in the case of Co(II) complex which are attributable to $^4T_1g \rightarrow {}^4A_2g(P)$ and $^4T_1g \rightarrow {}^4A_2g(F)$ transition respectively. These strongly suggest the formation of perfect octahedral geometry in the complexes (17,29). The magnetic susceptibility measurement revealed that the copper-containing complex 1 has effective magnetic moments of 2.00 B.M., which further confirm its octahedral geometry. The effective magnetic moment of 3.29 B.M. was obtained for the Ni(II) complexes thus, strengthen the octahedral geometry suggested for Ni(II) complexes with two unpaired electrons. The electronic spectra of the aqueous solution of Co(II) complexes of EHM showed three bands corresponding to the electronic transition of d^7 high spin octahedral geometry. The magnetic moment of 4.07 B.M. established for Co(II) complexes of EHM are in agreement with high spin octahedral (with three unpaired electrons) Co(II) complexes (29,30). The magnetic moments in the range of 2.00 – 4.07 B.M. further buttress the argument for the formation of octahedral complexes between Cu(II), Ni(II) and Co(II) transition metal ions and the EHM ligand (17).

Table 4: Molar conductivity, electronic spectra and magnetic susceptibility of metal complexes.

Compound	Molar Conductivity (Λ) Scm^2mol^{-1}	μ_{eff}(B.M)	λ_{max} (nm)	$\bar{\upsilon}$ (cm^{-1})	Assignments
Complex 1	155	2.00	280	35,714	n → π*
			650	15,384	$^2Eg \rightarrow {}^2T_{2g}$
Complex 2	387	3.29	280	35,714	n → π*
			373	26,810	$^3A_2g \rightarrow {}^3T_1g(P)$
			651	15,361	$^3A_2g \rightarrow {}^3T_1g(F)$
			991	10,091	$^3A_2g \rightarrow {}^3T_1g(F)$
Complex 3	362	4.07	295	33,898	n → π*
			485	20,619	$^4T_1g \rightarrow {}^4A_2g(P)$
			550	18,182	$^4T_1g \rightarrow {}^4A_2g(F)$
			680	14,706	$^4T_1g \rightarrow {}^4A_2g(F)$

Electrospray Ionization Mass Spectrometry (ESI-MS)

The major fragment ions, peaks assignment (theoretical and found), mass per charge ratio (m/z) and relative abundance of complex 3 is shown in Table 5. The fragment ions were formed by the addition of molecular adducts (mainly alkali metal and ammonium ions), formation of dimers and multiply charged ions which are characteristics nature of the technique. The m/z experimental values observed in each case compete satisfactorily well with the theoretical values; an evidence which further support molecular formulation of metal complexes (1:2 metal-ligand chelate). The quasimolecular ion were obtained in each case by the following fragment ions: $[M+NH_4+K]^+$, m/z = 588.10/586.06 (Fig. 3). Although, the ESI-MS analyses for complexes 1 and 2 could not be accomplished for a fair test due to the contaminations found in the samples possibly developed during the course of packaging for transportation, however, the presence of peak at m/z = 183.10 in all the spectra of complex 3 signify the involvement of EHM in the coordination sphere.

Table 5: ESI-MS data for $[Co(EHM)_2(H_2O)_2]Cl_2$.

Compound	Major Fragment Ions	Peak (m/z) Found	Assignment Theoretical	Relative intensity (%)
$[Co(EHM)_2(H_2O)_2]Cl_2$ $^m/_z$ = 529.05	$[M + NH_4 + K]^+$	588.10	586.06	0.63
	$[M + H + Li]^+$	537.10	537.09	5.70
	$[M + Li + Na]^+$	559.10	559.07	16.46
	$[M - 2H_2O + Li]^+$	500.10	500.06	39.24
	$[Co(EHM)_2(H_2O)(Cl) + 2Na]^{2+}$	261.10	261.03	36.08
	$[Co(EHM)Cl + K + Na]^+$	338.00	337.94	100.00
	$[2EHM + 2H]^{2+}$	183.10	183.09	16.46
	$[2EHM + Co + Na + 2H]^{2+}$	224.50	224.06	6.33
	$[2EHM+Co + H_2O + H + 2Na]^{2+}$	244.50	244.05	7.59

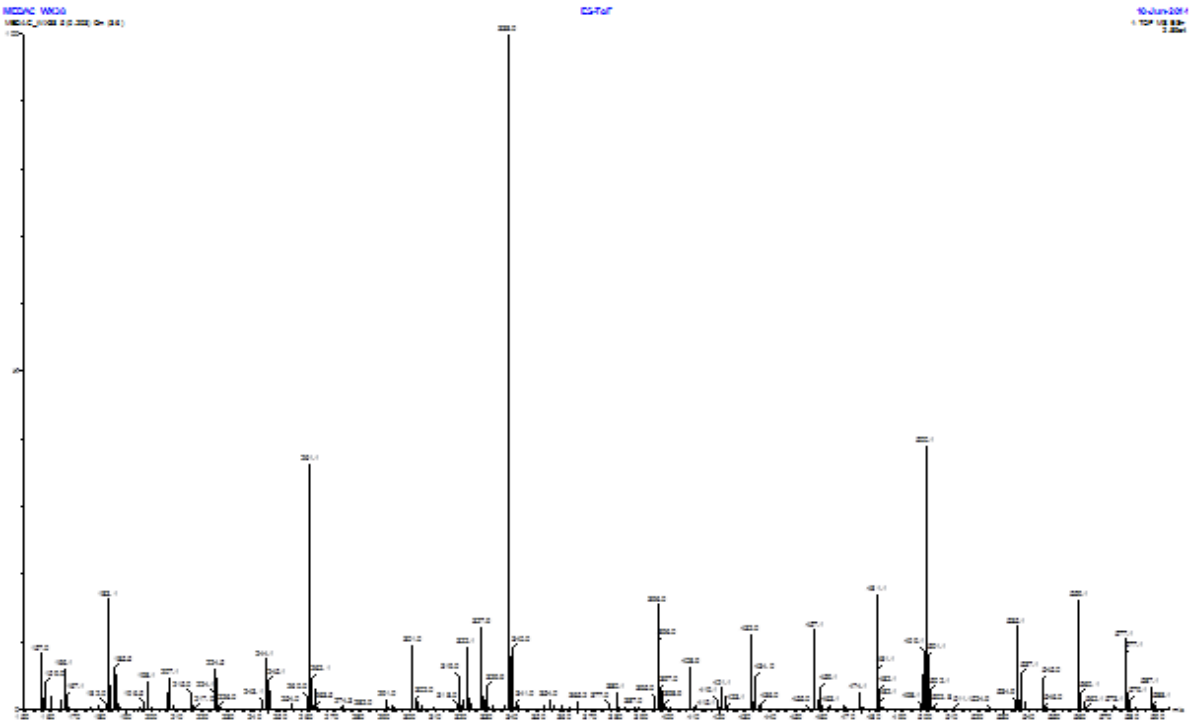


Figure 6: ESI-MS spectrum of complex 3.

The bioactivity profiles of the complexes are predicted *in silico* in comparison with the parent ligand, EHM in order to observe the possibility of enhanced pharmacology due to coordination (Table 6). The interaction with major targets for essential biofunctionalities such as the GPCR, ion channel, kinases, nuclear receptor, protease and enzymes are evaluated in terms of binding affinity. All the complexes virtually demonstrate competitive/higher binding affinity against the receptors than the parent EHM with exceptions to GPCR and protease where the ligand binds stronger. The theoretical interactions with these targets further support their applicability as bioactive agents (17).

Table 6: Predicted bioactivity profile of EHM and its complexes.

Compound	GPCR Ligand	Ion Channel Modulator	Kinase Inhibitor	Nuclear Receptor Ligand	Protease Inhibitor	Enzyme Inhibitor
EHM	0.01	0.19	-0.78	-0.72	0.14	-0.08
Complex 1	0.20	0.01	-0.07	0.00	0.20	0.09
Complex 2	0.16	0.08	0.02	0.10	0.28	0.04
Complex 3	0.22	0.11	0.05	0.12	0.36	0.05

The physicochemical parameters predicted for both the ligand, EHM and its metal complexes are presented (Table 7). Only the ligand EHM and complex 3 possess a Mol.wt <500, others are higher due to the nature of coordination with the metal ions and other ligands. They all soluble in water with fair molar refractivity, have hydrogen bond donor (HBD) groups ≤5 except complex 3 but higher number of hydrogen bond acceptors (HBA) than 10 except the ligand. They display topological polar surface area (TPSA) >60Å standard including the parent ligand possibly due to their structural morphology.

Table 7: Physicochemical properties of EHM and its complexes.

Compound	Mol.wt	Fraction Csp3[a]	HBA[b]	HBD[c]	Molar Refractivity	Water Solubility	TPSA[d] (Å²)
EHM	236.64	0.83	7	4	48.30	Highly soluble	98.57
Complex 1	521.31	0.83	15	4	95.48	Soluble	183.75
Complex 2	537.09	0.75	16	4	103.29	Soluble	181.30
Complex 3	455.27	0.83	14	6	85.48	Very soluble	147.16

a: The ratio of sp^3-hydridized carbon over the total number of carbon atoms in a molecule; b: The number hydrogen bond acceptors; c: The number of hydrogen bond donors; d: Topological polar surface area

The predicted pharmacokinetic profiles of the ligand, EHM and its complexes (Table 8) indicate that all the complexes have low ability for gastrointestinal absorption compared to the ligand. None of them including the parent ligand can predictably penetrate the blood brain barrier (BBB), inhibit the cytochrome P450, indicating their insignificance for drug-drug interaction to induce adverse effects. They all possess low skin permeation indicated by Log Kp value of -9.58 to -8.33 cm/s and are P-G substrates except the ligand. Although, some of them show slight violations to the Lipinski's Rule of 5 (31) for drugability due to higher molecular weights than 500 g/mol commonly to coordination compounds (17,32), however they demonstrate good pharmacokinetics and bioavailability for further bioactivity probes.

Table 8: Pharmacokinetics properties of EHM and its complexes.

Compound	GI Abs.[a]	BBB Permeation[b]	P-G Substrate[c]	CYP1A2 Inhibitor[d]	LogKp[e] (cm/s)
EHM	High	No	No	No	-9.58
Complex 1	Low	No	Yes	No	-8.33
Complex 2	Low	No	Yes	No	-9.19
Complex 3	Low	No	Yes	No	-9.51

a: The ratio of sp3 hydridized carbon over the total number of carbon atoms in a molecule; b: The number hydrogen bond acceptors; c: The number of hydrogen bond donors; d: Topological polar surface area

The zones of inhibitions shown in Fig. 4 indicate that the metal complexes exhibit stronger inhibition effects on the test organisms than the parent ligand and in good competition with a renown antibiotic, ciprofloxacin *in vitro*. It has also been observed that antibacterial potency in each case appears to be concentration-dependent as the degree of inhibition increases with increase in concentration (30, 33). The complexes inhibit the bacterial growth at similar minimal bactericidal concentration and in strong competition with a renowned antibiotic for treating bacterial resistance, ciprofloxacin. The improved activity of the metal-drug chelates can be justified on the basis of chelation effect (34) and it indicates the worthiness of the complexes for therapeutic transformations against drug-resistant antibacterial upon further studies.

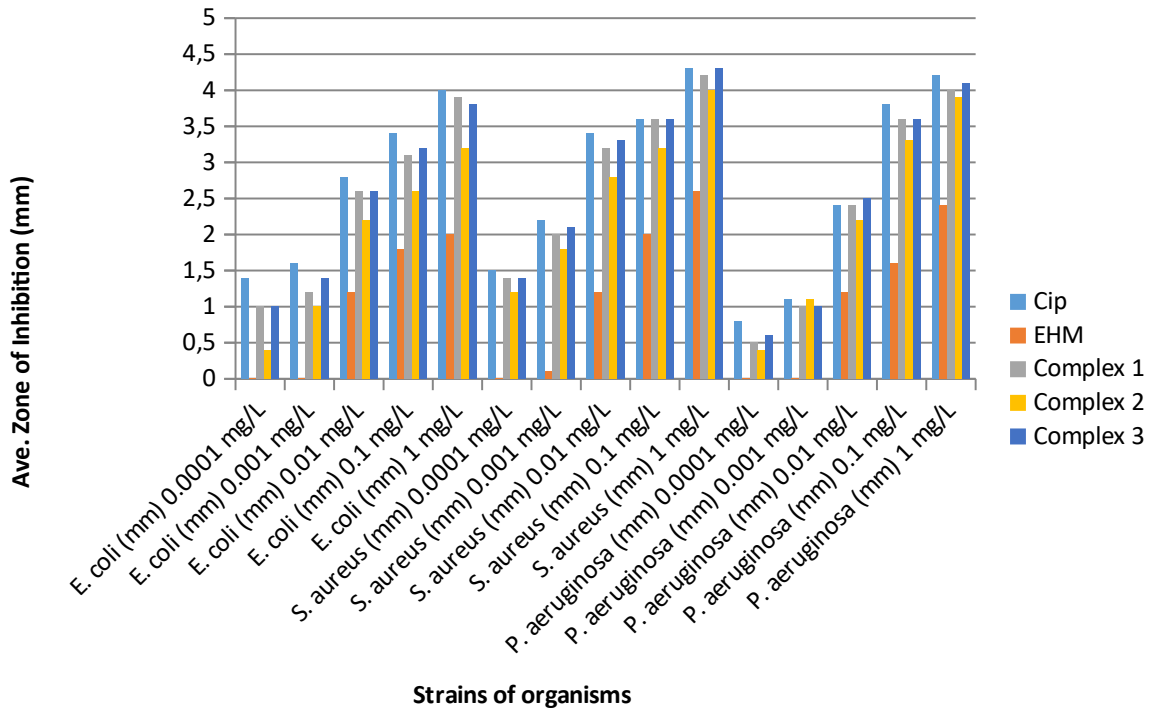


Figure 7: Comparative effect of inhibitory level of the ligand and metal complexes on *E. coli, S. aureus and P. aeroginosa* at different concentrations (mgL^{-1})

CONCLUSION

New eflornithine hydrochloride monohydrate-metal(II) complexes were synthesized with oxygen, nitrogen and chloride donor atoms by 1:2 molar condensation of metal ions and the ligand. The ligand and the metal complexes were characterized using elemental analysis, FT-IR, electronic spectra, magnetic susceptibility and ESI-MS. Eflornithine hydrochloride monohydrate acted as a bidentate ligand in each case, coordinating to the metal ion through the carboxylate oxygen atom and amine nitrogen atom and octahedral geometry is reasonably proposed for all the metal complexes based on the characterization results. Metal(II) complexes of the ligand showed enhanced antibacterial activity than the free ligand and compete favorably well with a renowned antibiotic, ciprofloxacin, indicating that the metal complexes are potentially good antibacterial agent. It has also been observed that degree of inhibition is concentration dependent as the activity increased with increased concentration. Although, the complexes could not be achieved in single crystal forms after several recrystallization attempt and more robust characterization and biological assays are required for more accurate elucidation, however, the study presents fundamentals amenable for therapeutic development in form of divalent metal complexes of EHM against drug-resistant bacteria.

ACKNOWLEDGMENTS

The authors gratefully acknowledge the financial support from the World Bank Science and Technology Education Post-Basic Project (STEP-B) TETFUND, Department of Chemistry University of Ilorin, Nigeria and also Tetfund Nigeria for PhD scholarship awarded to YOA.

REFERENCES

1. Jing L, Dejuan S, Yueying Y, Mingxue L, Hua L, Lixia C. Discovery of metal-based complexes as promising antimicrobial agents. Discovery of metal-based complexes as promising antimicrobial agents. European Journal of Medicinal Chemistry. 2021; 224, 113696:1-14. <URL>.

2. Raman N, Sobha S, Mitu L. Synthesis, structure elucidation, DNA interaction, biological evaluation, and molecular docking of an isatin-derived tyramine bidentate Schiff base and its metal complexes. Monatshefte Fur Chemie. 2012;143:1019–30. <URL>.

3. Saddam Hossain Md, Zakaria CM, Kudrat-E-Zahan Md. Metal Complexes as Potential Antimicrobial Agent: A Review. American Journalof Heterocyclic Chemistry. 2018, 4(1):1-21.<URL>.

4. Ayipo YO, Osunniran WA, Babamale HF, Ayinde MO, Mordi MN. Metalloenzyme mimicry and modulation strategies to conquer antimicrobial

resistance: Metal-ligand coordination perspectives. Coordination Chemistry Review 2022;453:214317. <URL>.

5. Frei A. Metal complexes, an untapped source of antibiotic potential. Antibiotics. 2020; 9(2) :1-25 <URL>.

6. Tella AC, Obaleye JA. Metal complexes as antibacterial agents : Synthesis , characterization and antibacterial activity of some 3d metal complexes of sulphadimidine. Electronic Journal of Chemistry. 2010;2(1):1–16.

7. Anacona JR, Ortega G. Metal-based antibacterial agents: Synthesis, characterization, and biological evaluation of ternary Mn(II) and Co(II) complexes containing sulfamethoxazole and cephalosporins. Synthesis and Reactivity in Inorganic, Metal-Organic, and Nano-Metal Chemistry. 2015;45(3):363– 69 <URL>.

8. Abdullahi OR, Halimah FB, Amudat L, Abdulbasit AA, Wahab AO, Ayinla, OS, Misitura L, Joshua AO. Mn(II), Co(II), Ni(II), And Cu(II) Complexes Of Amıno Acıd Derıved Schıff Base Lıgand: Synthesıs, Characterızatıon And *In-vıtro* Antıbacterıal Investıgatıons. Bull. Chem. Soc. Ethiop. 2021; 35(1): 97-106. <URL>.

9. Ikmeet K, Sukhbir S, Sandeep A, Neelam S. Application of Central Composite Design for Development and Optimization of Eflornithine Hydrochloride-loaded Sustained Release Solid Lipid Microparticles. Biointerface Research in Applied Chemistry. 2022; 12(1): 618-37 <URL>.

10. Amit K, Vijender S, Praveen K. Spectrophotometric Determination of Eflornithine Hydrochloride using Vanillin as Derivative Chromogenic Reagent. Tropical Journal of Pharmaceutical Research. 2014; 13 (11): 1917-23. <URL>.

11. Ikmeet KG, Sukhbir S, Sandeep A, Neelam S. Development And Validatıon Of Uv-Spectrophotometer Analytical Method Of Eflornithıne Hydrochlorıde. Plant Archives. 2020; 20(1), 3265-70

12. Osunniran WA, Obaleye JA, Tella AC, Amolegbe SA. Synthesis, characterization and in vitro antibacterial studies of novel transition metal(II) complexes of 2,5-diamino-2-(difluoromethyl)pentanoic acid hydrochloride hydrate. Orbital. 2018;10:367– 380. <URL>.

13. Obaleye JA, Tella AC, Osunniran WA, Simon N, Omojasola PF. Synthesis, Characterization, Crystal Structure and Antimicrobial Evaluation of a Novel -M-X-M-X- Type Infinite Chain 1D Cu(II) Complex with Eflornithine Hydrochloride Hydrate as Ligand. *J Inorg Organomet Polym Mater.* 2014; 24:827–35. <URL>.

14. Osunniran WA, Obaleye JA, Ayipo YO. Six Coordinate Transition Metal(II) Complexes of Mixed Ligands of Eflornithine Hydrochloride Hydrate and 2,2-Bipyridine: Synthesis, Characterization and Antibacterial Study. Jordan Journal Chemistry. 2018;13:149–57.

15. Barman Balfour JA, McClellan K. Topical Eflornithine. American Journal of Clinical Dermatology. 2001; 2(3): 197-201

16. Daina A, Michielin O, Zoete V. SwissADME: A free web tool to evaluate pharmacokinetics, drug-likeness and medicinal chemistry friendliness of small molecules. *Sci Rep* 2017;7:1–13. <URL>.

17. Okasha RM, Al Shaikh NE, Aljohani FS, Naqvi A, Ismail EH. Design of novel oligomeric mixed ligand complexes: Preparation, biological applications and the first example of their nanosized scale. International Journal of Molecular Science. 2019; 20(3),743. <URL>.

18. Ayipo YO, Obaleye JA, Badeggi UM. Novel Metal Complexes of Mixed Piperaquine-Acetaminophen and Piperaquine-Acetylsalicylic acid : Synthesis, Characterization and Antimicrobial Activities. Journal of Turkish Chemical Society A. 2017;4:313–26. <URL>.

19. Limbago B. M100-S11, Performance standards for antimicrobial susceptibility testing. Clin Microbiol Newsl. 2019;23(6): 23-49. <URL>.

20. Osunniran WA, Obaleye JA , Tella AC , Ayipo YO, Bale AT, Rajee AO. Toxıcologıcal Assessment Of Synthesızed And Characterızed Transıtıon Metal(II) Complexes Of Eflornıthıne Hydrochlorıde Hydrate On Albıno Rats. Bull. Chem. Soc. Ethiop. 2020; 34(3), 489-50. <URL>.

21. Rajee AO, Aliyu AA , Babamale HF, Lawal A, Ayinla SO, Osunniran WA, Obaleye JA. Preparation, characterization and antibacterial activity of Mn(II), Cu(II) and Zn(II) complexes of methionine and 2,2-bipyridine co-ligands. Journal of the Kenya Chemical Society. 2020; 13(1): 16-21.

22. Modec B, Podjed N, Lah N. Beyond the simple copper(II) coordination chemistry with quinaldinate and secondary amines. Molecules. 2020; 25(7), 1573. <URL>.

23. Karthik P, Shaheer ARM, Vinu A, Neppolian B. Amine Functionalized Metal–Organic Framework

Coordinated with Transition Metal Ions: d–d Transition Enhanced Optical Absorption and Role of Transition Metal Sites on Solar Light Driven H2 Production. Small. 2020;16(12):1–10. <URL>.

24. Turan N, Buldurun K. Synthesis, characterization and antioxidant activity of Schiff base and its metal complexes with Fe(II), Mn(II), Zn(II), and Ru(II) ions: Catalytic activity of ruthenium(II) complex. European Journal of Chemistry. 2018; 9(1):22–9. <URL>.

25. Tadewos D, Digafie Z, Tegene D, Demissie TB, Eswaramoorthy R. Synthesis, Characterization, and Biological Activities of Novel Vanadium(IV) and Cobalt(II) Complexes, *ACS Omega* 2022;, 7(5) : 4389–404. <URL>.

26. Salazar-Medina AJ, Gámez-Corrales R, Ramírez JZ, González-Aguilar GA, Velázquez-Contreras EF. Characterization of metal-bound water in bioactive Fe(III)-cyclophane complexes. Journal of Molecular Structure. 2018;1154:225–31. <URL>.

27. Osunniran WA, Ayipo YO, Adeyemo MA, Bale AT, Obaleye, JA. Comparison of Solid and Solvent - Based Syntheses, Characterization and Antioxidant Property of Metal Complexes of Sodium Diclofenac, Fountain Journal of Natural and Applied Science. 2020; 9(1): 11-18. <URL>.

28. Wail AZ, Abbas A, Salih A, Susan DA, Young GK. Synthesis, characterization, and biological activity of Schiff bases metal complexes. Journal of Physical Organic Chemistry. 2017; 31(2) e3752:1-13. <URL>.

29. Srivastava VK. Synthesis, characterization, and biological studies of some biometal complexes. Future Journal of Pharmaceutical Sciences. 2021; 7(51):1-11. <URL>

30. Obaid SMH, Jarad AJ, Salih AA. Synthesis, Characterization and Biological Activity of Mixed Ligand Metal Salts Complexes with Various Ligands. Journal of Physics: Conference Series, 2020; 1660, 012028: 1-14. <URL>.

31. Lipinski CA. Lead- and drug-like compounds: The rule-of-five revolution. Drug Discov Today Technol. 2004;1(4):337– 41. <URL>.

32. Syed AFS, Paulpandiyan R, Nagarajan ER. Expatiating biological excellence of aminoantipyrine derived novel metal complexes: Combined DNA interaction, antimicrobial, free radical scavenging studies and molecular docking simulations. Journal of Molecular Structure. 2019;1178:179–91. <URL>

33. Kuti JL. Optimizing Antimicrobial Pharmacodynamics: a Guide for Your Stewardship Program. Rev Médica Clínica Las Condes. 2016; 27(5):615–24. <URL>.

34. Coraça-Huber D, Dichtl S, Steixner S, Nogler M, Weiss G. Iron chelation destabilizes bacterial biofilms and potentiates the antimicrobial activity of antibiotics against coagulase-negative Staphylococci. Pathogens and Disease. 2018; 76(5):1-8. <URL>.